Supplementary Materials for

A new perspective on the hydraulics of oilfield wastewater disposal: How PTX conditions affect fluid pressure transients that cause earthquakes

Ryan M. Pollyea*[,a], Graydon L. Konzen[a], Cameron C. Chambers[a], Jordan A. Pritchard[a], Hao Wu[a], and Richard S. Jayne[a,b]

[a] *Department of Geosciences, Virginia Polytechnic Institute & State University, Blacksburg, VA 24061, USA*
[b] Present Address: *Applied Systems Analysis and Research Department, Sandia National Laboratory, Albquerque, New Mexico, USA*

*Correspondence to: rpollyea@vt.edu

This Electronic Supplement includes:

- Supplemental Text: Summary of TOUGH3 Governing Equations.
- Figure S1: Time-series simulation data below injection well at 5 km depth for wastewater comprising 207,000 ppm TDS at 10°, 25°, and 40°C.
- Figure S2: Time-series simulation data below injection well at 5 km depth for wastewater at 25°C with fluid composition comprising 107,000, 157,000, and 207,000 ppm TDS.
- Figure S3: Time-series simulation data at 4.5 km depth and 4 km radial distance from well for wastewater comprising 207,000 ppm TDS at 10°, 25°, and 40°C.
- Figure S4: Time-series simulation data at 4.5 km depth and 4 km radial distance from well for wastewater at 25°C with fluid composition comprising 107,000, 157,000, and 207,000 ppm TDS.

Summary of TOUGH3 Governing Equations

The code selection for this study is TOUGH3 [3] compiled with equation of state module EOS7 for simulating non-isothermal mixtures of water and brine with mixing by advective transport and Fickian diffusion. The TOUGH3 simulator solves the conservation equations for mass and energy flow in porous geologic media. The complete solution scheme is presented in the TOUGH3 User's

Guide [2], and we summarize the governing equations in the context of fully saturated flow here. The general form of mass- and energy conservation equation is written as:

$$\frac{d}{dt}\int_{V_n} M^\kappa dV_n = \int_{\Gamma_n} \mathbf{F}^\kappa \cdot \mathbf{n} d\Gamma_n + \int_{V_n} q^\kappa dV_n \tag{1}$$

In this formulation, the left side of Equation 1 is the accumulation term, where M represents a mass (or energy) component κ, which for this study are pure water, brine and energy (in which case κ is specific inner energy). As a result, the time-change of mass (or energy) within closed volume V_n is equivalent to the sum of (1) the integral component flux ($\mathbf{F}^\kappa$) normal to the volume-bounding surface (Γ_n) and (2) any sources or sinks (q^κ) of component κ within V_n.

The mass accumulation term in equation 1 is generalized as:

$$M^\kappa = \phi \sum S_\beta \rho_\beta X_\beta^\kappa, \tag{2}$$

where, ϕ is porosity, S_β is the saturation of phase β (only aqueous phase is considered in this study), ρ_β is density of phase β, X_β^κ is mass fraction of mass component κ in phase β. In Equation 2, M^κ is summed over all fluid phases occupying pore space in V_n; however, for this study, we are only considering fully saturated flow. To solve for nonisothermal conditions, the heat accumulation term, is given by:

$$M^\kappa = (1-\phi)\rho_R C_R T + \phi \sum S_\beta \rho_\beta u_\beta. \tag{3}$$

In Equation 3, ρ_R is rock density, C_R is rock specific heat, T is temperature, and u_β is enthalpy of phase β. In TOUGH3, the advective flux ($\mathbf{F}^\kappa|_{\text{adv}}$) for each mass component κ is given as the sum of all phase fluxes, $\mathbf{F}^\kappa|_{\text{adv}} = \sum X_\beta^\kappa \mathbf{F}_\beta$, where $\mathbf{F}_\beta$ is presented here in terms of Darcys Law for fully saturated porous media:

$$\mathbf{F}_\beta = -\frac{k\rho\beta}{\mu_\beta}(\nabla P_\beta - \rho_\beta \mathbf{g}), \tag{4}$$

where, k is intrinsic permeability, μ_β is dynamic viscosity of phase β, P_β is fluid pressure of phase β, and $\mathbf{g}$ is the vector of gravitational acceleration. Diffusive mass transport ($\mathbf{f}^\kappa$) is modeled as,

$$\mathbf{f}^\kappa = -\phi\tau_0\tau_\beta\rho_\beta D_\beta^\kappa \nabla X_\beta^\kappa, \tag{5}$$

where, $\tau_0\tau_\beta$ is the tortuosity coefficient (not considered in our models) and D_β^κ is the diffusion coefficient for mass component κ in phase β. Our models consider injection wells as source terms in the relevant grid cells. To convert from volume rate (Q) to mass rate ($\dot{m}$), we use the standard conversion, $\dot{m} = Q\rho$, where ρ is the injection fluid density at reservoir temperature and pressure.

The governing equations are solved by the integral finite difference method for space discretization, while time discretization is fully implicit, first-order backward finite difference. This results in a coupled, nonlinear set of equations that are solved simultaneously by Newton-Raphson iteration. During nonisothermal simulation, the temperature dependence on properties of pure water are calculated internally from the steam equations.

To account for brine properties as a function of PTX conditions, we implement the TOUGH3 equation of state module for aqueous mixtures of pure water and brine, EOS7 [4]. In this formulation, aqueous phase salinity is accounted for on the basis of a brine mass fraction, X_b, for which density and viscosity are interpolated between end-members comprising pure water and brine. Although the code makes allowances for unsaturated conditions, we consider only fully saturated flow in this study, and, as a result, our models obviate problems that may be encountered during phase change (e.g., salting out effects). The fundamental assumption in EOS7 is that fluid volume is conserved during mixing of water and brine [1]. As a result, the density of the water-brine mixture (ρ_m) for variable brine saturation (X_b) can be approximated as,

$$\frac{1}{\rho_m} = \frac{1 - X_b}{\rho_w} + \frac{X_b}{\rho_b}, \tag{6}$$

where, ρ_w is the density of pure water and ρ_b is the density of a reference brine when X_b is one. For our study, the reference brine density is 1,123 kg/m^3. The approximation for density of the brine-water mixture (equation 6) further assumes the compressibility of brine to be the same as for pure water. To account for the effects of pressure, temperature, and salinity on the viscosity of the brine-water mixture (μ_m), the polynomial correction by Herbert [1] is invoked as:

$$\mu_m(P, T, X) = \mu_w(P, T)[1 + 0.4819X_b - 0.2774X_b^2 + 0.7814X_b^3], \tag{7}$$

where, μ_w is the viscosity of pure water, for which temperature and pressure dependence is calculated for by internally referencing the equation of state for water.

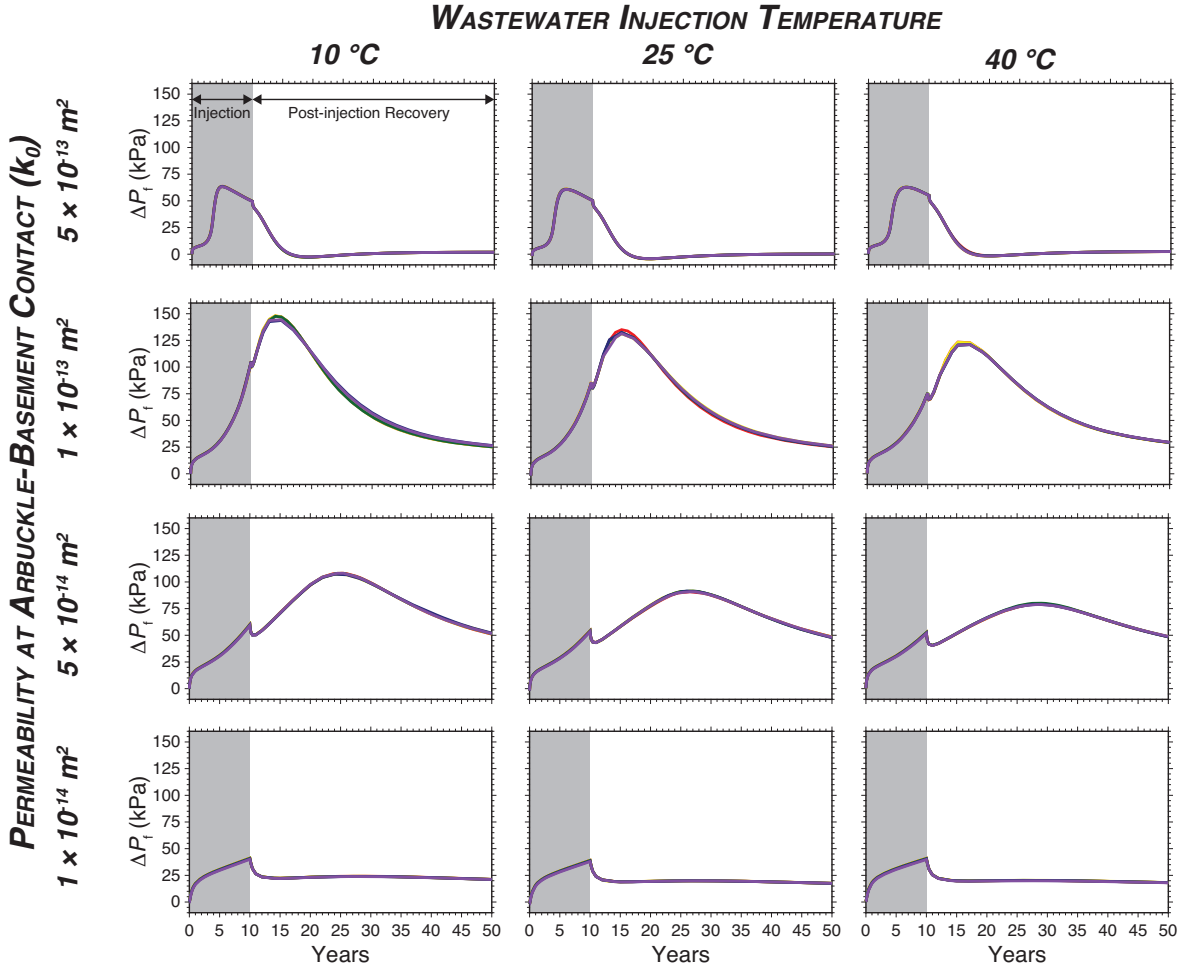

Figure S1: Time series of fluid pressure change (ΔP_f) below the injection well at 5 km depth for all model scenarios with wastewater comprising 207,000 ppm TDS at 10°, 25°, and 40°C. Each panel is a unique combination of permeability at the Arbuckle-basement contact and wastewater injection temperature – the curves on each panel correspond with the six basement fracture compressibility values tested for this study (β_f): 1×10^{-9} Pa^{-1} (purple), 5×10^{-10} Pa^{-1} (blue), 1×10^{-10} Pa^{-1} (green), 5×10^{-11} Pa^{-1} (yellow), 1×10^{-11} Pa^{-1} (orange) and 5×10^{-12} Pa^{-1} (red). Note that there is little separation between curves because fluid ΔP_f is insensitive to basement fracture permeability.

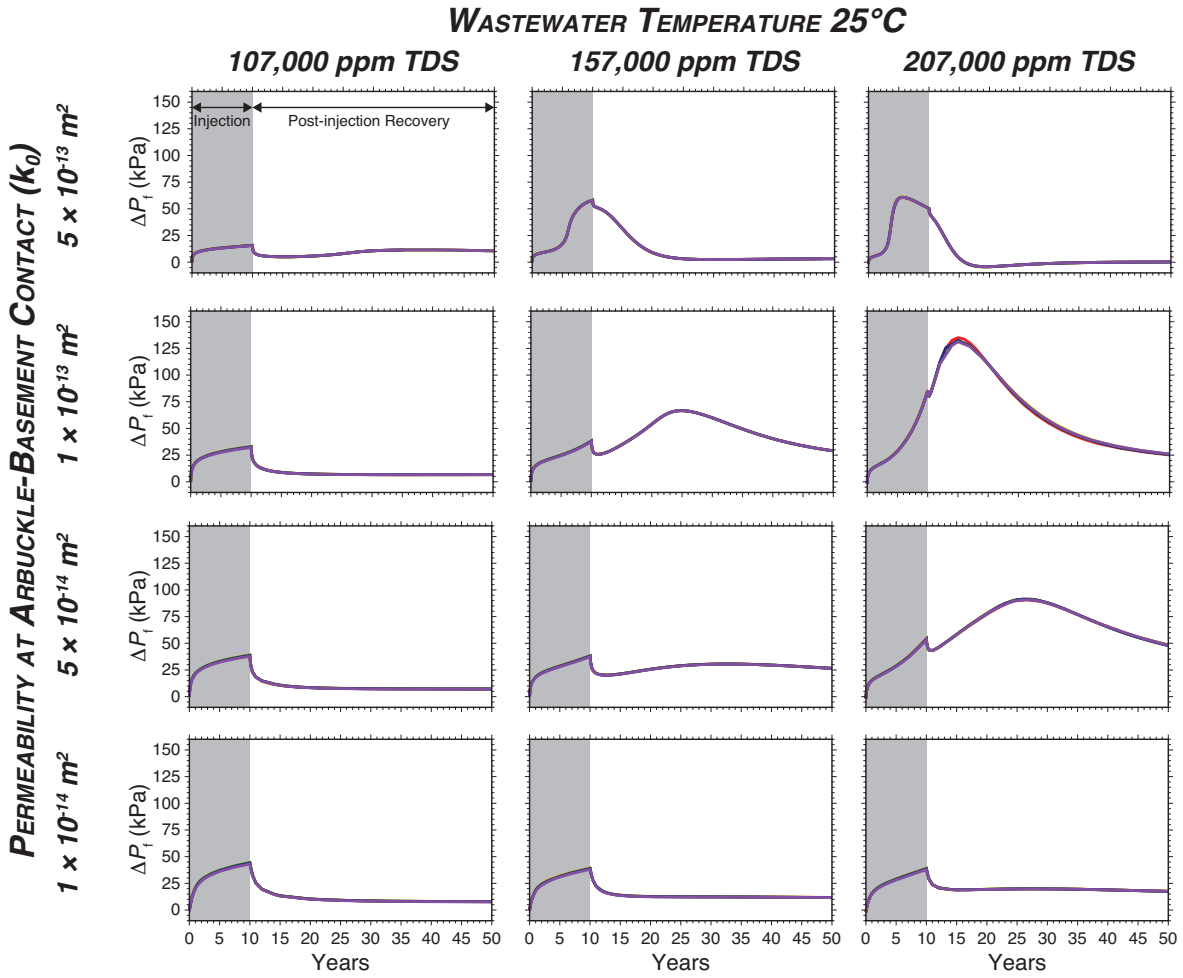

Figure S2: Time series of fluid pressure change (ΔP_f) below the injection well at 5 km depth for all model scenarios with wastewater at 25°C with fluid composition comprising 207,000, 157,000, and 107,000 ppm TDS. Each panel is a unique combination of permeability at the Arbuckle-basement contact and wastewater injection temperature – the curves on each panel correspond with the six basement fracture compressibility values tested for this study (β_f): 1×10^{-9} Pa^{-1} (purple), 5×10^{-10} Pa^{-1} (blue), 1×10^{-10} Pa^{-1} (green), 5×10^{-11} Pa^{-1} (yellow), 1×10^{-11} Pa^{-1} (orange) and 5×10^{-12} Pa^{-1} (red). Note that there is little separation between curves because fluid ΔP_f is insensitive to basement fracture permeability.

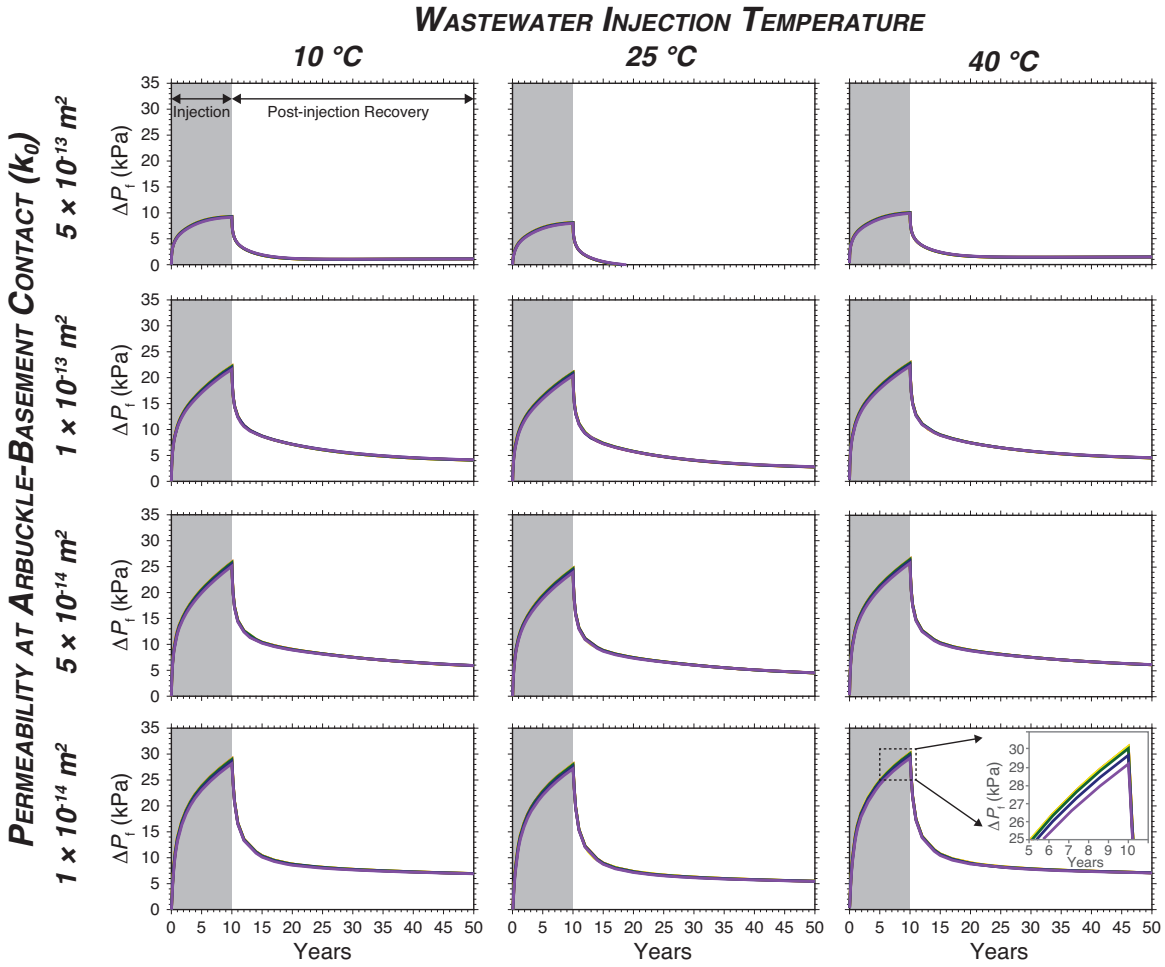

Figure S3: Time series of fluid pressure change (ΔP_f) below the injection well at 4.5 km depth and 4 km radial distance from the injection well for all model scenarios with wastewater comprising 207,000 ppm TDS at 10°, 25°, and 40°C. Each panel is a unique combination of permeability at the Arbuckle-basement contact and wastewater injection temperature – the curves on each panel correspond with the six basement fracture compressibility values tested for this study (β_f): 1×10^{-9} Pa^{-1} (purple), 5×10^{-10} Pa^{-1} (blue), 1×10^{-10} Pa^{-1} (green), 5×10^{-11} Pa^{-1} (yellow), 1×10^{-11} Pa^{-1} (orange) and 5×10^{-12} Pa^{-1} (red). There is little separation between curves because fluid ΔP_f is insensitive to basement fracture permeability except when wastewater temperature is 40°C and k_0 is 1×10^{-14} m^2 (lower right panel).

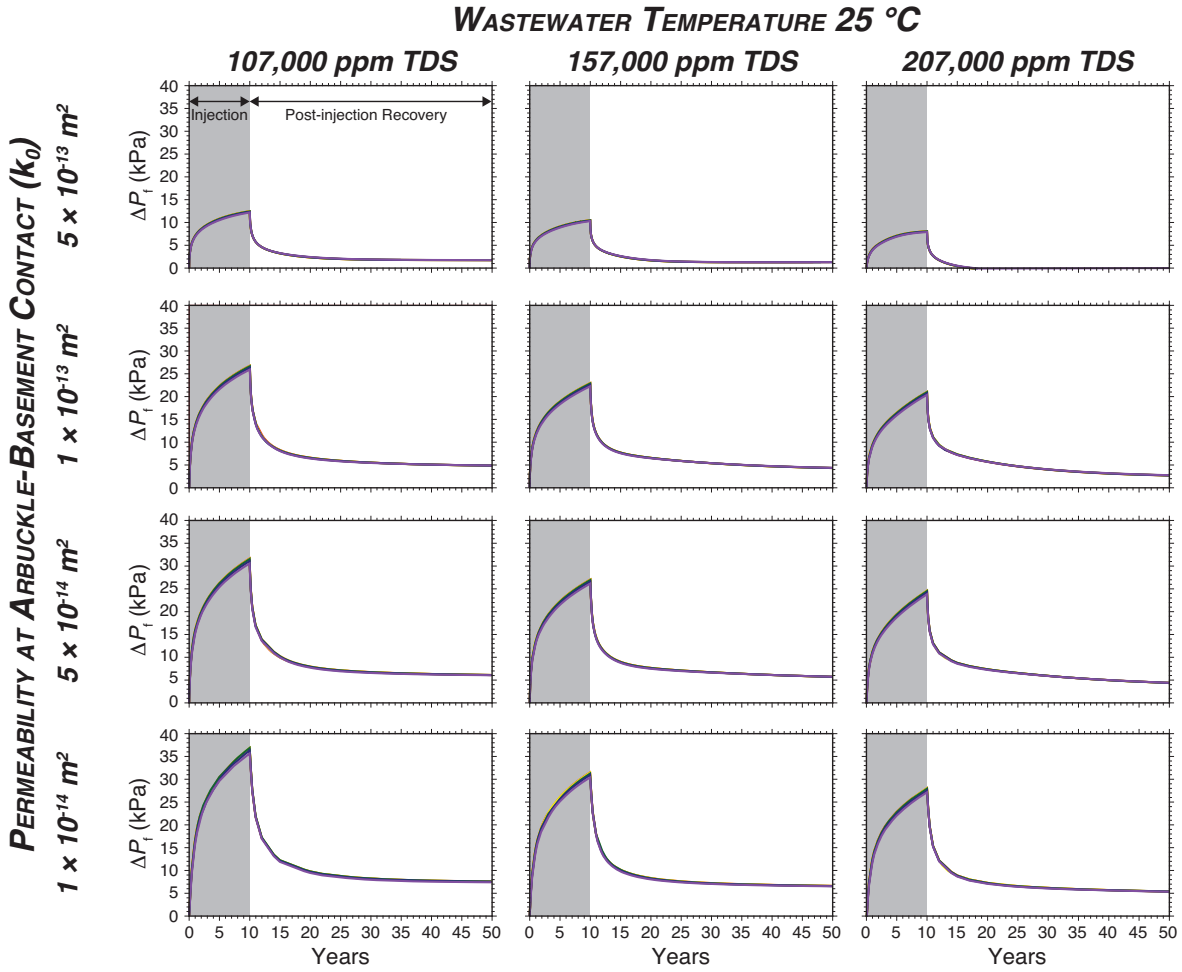

Figure S4: Time series of fluid pressure change (ΔP_f) below the injection well at 4.5 km depth and 4 km radial distance from the injection well for all model scenarios with wastewater at 25°C with fluid composition comprising 207,000, 157,000, and 107,000 ppm TDS. Each panel is a unique combination of permeability at the Arbuckle-basement contact and wastewater injection temperature – the curves on each panel correspond with the six basement fracture compressibility values tested for this study (β_f): 1×10^{-9} Pa^{-1} (purple), 5×10^{-10} Pa^{-1} (blue), 1×10^{-10} Pa^{-1} (green), 5×10^{-11} Pa^{-1} (yellow), 1×10^{-11} Pa^{-1} (orange) and 5×10^{-12} Pa^{-1} (red). Note that there is little separation between curves because fluid ΔP_f is insensitive to basement fracture permeability.

References

[1] AW Herbert, CP Jackson, and DA Lever. Coupled groundwater flow and solute transport with fluid density strongly dependent upon concentration. *Water Resources Research*, 24(10):1781–1795, 1988.

[2] Yoojin Jung, George Shu Heng Pau, Stefan Finsterle, and Christine Doughty. TOUGH3 User's

Guide: Version 1.0. Technical report, Lawrence Berkeley National Laboratory, 2018. LBNL-2001093.

[3] Yoojin Jung, George Shu Heng Pau, Stefan Finsterle, and Ryan M Pollyea. TOUGH3: A new efficient version of the TOUGH suite of multiphase flow and transport simulators. *Computers & Geosciences*, 108:2–7, 2017.

[4] Karsten Pruess, Curt Oldenburg, and George Moridis. TOUGH2 User's Guide, Version 2. Technical report, Lawrence Berkeley National Laboratory, November 1999. LBNL-43134.